European Journal of Medicinal Chemistry 44 (2009) 1959–1971

Contents lists available at ScienceDirect

European Journal of Medicinal Chemistry

journal homepage: http://www.elsevier.com/locate/ejmech

Original article

Synthesis, pharmacological evaluation and docking studies of new sulindac analogues

Nelilma C. Romeiro, Ramon D.F. Leite, Lidia M. Lima*, Suzana V.S. Cardozo, Ana L.P. de Miranda, Carlos A.M. Fraga, Eliezer J. Barreiro*

Laboratório de Avaliação e Síntese de Substâncias Bioativas (LASSBio), Faculdade de Farmácia, Universidade Federal do Rio de Janeiro (UFRJ), Rio de Janeiro, PO Box 68023, RJ 21944-970, Brazil

ARTICLE INFO

Article history:
Received 1 September 2008
Received in revised form
26 November 2008
Accepted 27 November 2008
Available online 6 December 2008

Keywords:
Molecular docking
Sulindac analogues
NSAIDs
Antinociceptive
Anti-inflammatory drugs

ABSTRACT

This paper describes the synthesis, pharmacological evaluation and docking studies of a series of new sulindac analogues. Overall, the designed compounds revealed good, in vivo, antinociceptive activity and satisfactory anti-inflammatory profile. Flexible molecular docking with COX-1/COX-2 has shown putative binding modes of the designed compounds while the theoretical evaluation of cell permeability based on Lipinski's rule of five has helped rationalize the biological results.

© 2008 Elsevier Masson SAS. All rights reserved.

1. Introduction

Prostaglandins act as potent mediators of pain, fever and inflammation. Prostaglandin H synthase (COX) catalyses the conversion of arachidonic acid to the prostaglandin endoperoxide PGG2 then PGH2, which serves as the precursor for the formation of PGs and thromboxanes [1,2]. Two isoforms of COX have been identified [3–5]. The first, COX-1, is constitutively expressed in most tissues and is believed to generate prostaglandins for normal physiological functions. The second isoform, COX-2, is characterized by a rapid induction by a variety of stimuli, including mitogens, hormones, cytokines, and growth factors. Selective inhibition of COX-2 is desirable in order to avoid gastric side effects generally associated with inhibition of COX-1, which is responsible for gastric mucosa protection [3–5].

Non-steroidal anti-inflammatory drugs (NSAIDs) [6,7] exert their anti-inflammatory, antipyretic and antinociceptive effects by blocking the production of prostanoids from arachidonic acid through inhibition of COX activity. Classic NSAIDs like sulindac (**1**) [8], aspirin (ASA, **2**) [9], meclofenamic acid (**3**) [10] and indomethacin (**4**) [11] (Fig. 1) inhibit both isoforms of COX non-selectively or with low selectivity, exerting their anti-inflammatory activity via inhibition of COX-2, and their deleterious side effects by inhibition of COX-1 (Fig. 1). In order to provide an effective treatment for inflammatory disorders, the design of selective inhibitors of COX-2 has been widely described as a new therapeutical approach, aiming at obtaining new NSAIDs, devoid of the side effects commonly associated with conventional NSAIDs [12–15].

Examples of selective inhibitors of COX-2 are celecoxib (**5**) [16], rofecoxib (**6**) [17], valdecoxib (**7**) [18] and etoricoxib (**8**) [19] (Fig. 1). Although rofecoxib (**6**, Fig. 1) has been withdrawn from the market because of its cardiovascular side effects originated from long-term treatment, and valdecoxib (**7**, Fig. 1) has been withdrawn for serious cutaneous adverse reactions, there still remains a lot of research work to be done in the design of new safer anti-inflammatory drugs, selective COX-2 inhibitors [20,21].

Additionally, the action of NSAIDs in other pathologies has been the subject of many studies. For instance, recent reports have shown a growing body of evidence that COX-2 expression is a fundamental step in breast cancer pathogenesis acting through prostaglandin-dependent and independent mechanisms [22,23]. Epidemiological studies suggest that NSAIDs confer a moderate degree of benefit against breast cancer [24–26]. Further reports

* Corresponding authors. Tel./fax: +55 21 2562 6644.
E-mail addresses: lidia@pharma.ufrj.br, ejbarreiro@ccsdecania.ufrj.br (L.M. Lima).

0223-5234/$ – see front matter © 2008 Elsevier Masson SAS. All rights reserved.
doi:10.1016/j.ejmech.2008.11.012

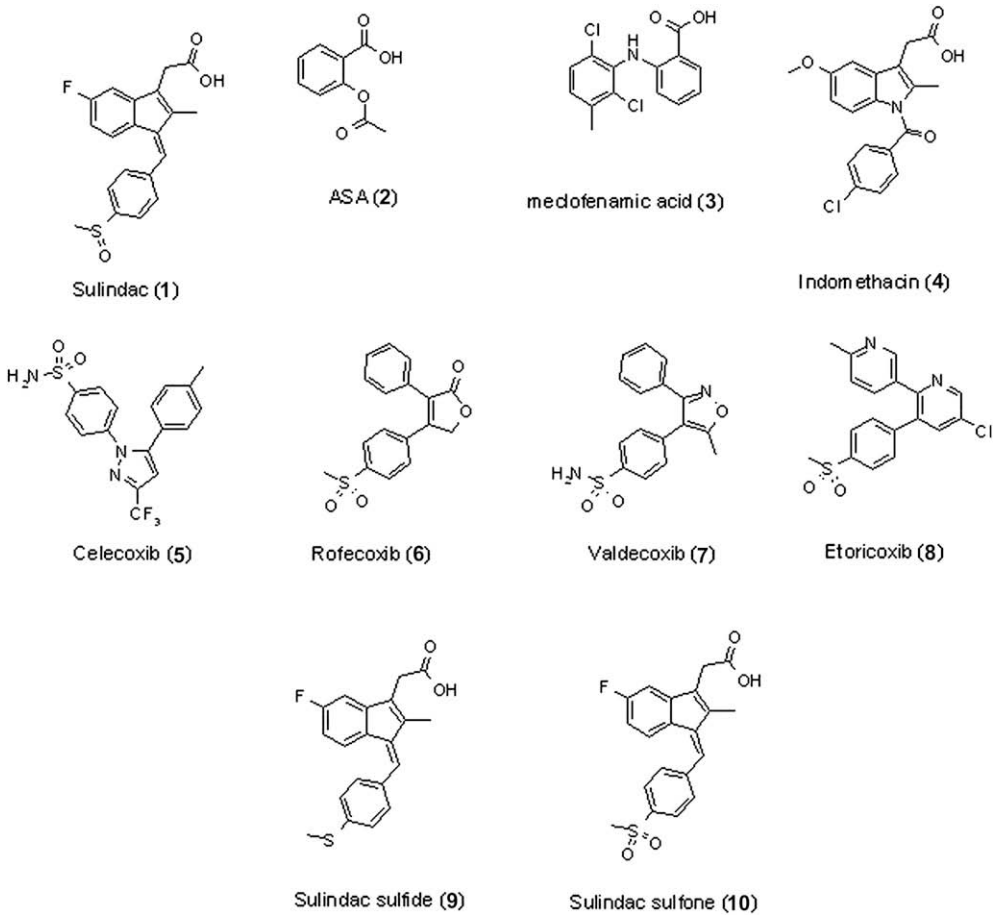

Fig. 1. NSAIDs, COX-1/COX-2 inhibitors.

have shown the ability of NSAIDs to prevent colorectal cancer, among other diseases [27–30]. However further work is required to establish how this enzyme system can be best manipulated for therapeutic benefit.

One of the existing approaches for the design of such substances is the molecular modification of existing drugs, e.g., second generation NSAIDs, which are comprised of modified classic NSAIDs [31–35]. This approach is based on the introduction of pharmacophores aiming at improving the selectivity for COX-2. Examples of this approach have been reported recently and include aspirin, indomethacin, flurbiprofen, ketoprofen and meclofenamic acid derivatives with improved selectivity to COX-2 [31–35]. Among these compounds, amide derivatives of indomethacin have shown great selectivity for COX-2, with a special performance of aliphatic amides with maximum of eight carbon atoms, secondary amides and terminally functionalized alkyl chains (Fig. 2) [31–33]. Among the preferred terminal groups in the ester functionalized chain, the benzyl radical with substituents in position 4 showed greater selectivity to COX-2. In the meclofenamic acid series, *O*-substituted hydroxamate derivatives and alkyl chains functionalized with a halogen atom showed greater selectivity among other modifications [34]. Successful examples of these compounds are shown in Fig. 2.

Sulindac analogues have been explored in our group as new potential anti-inflammatory agents using safrole, an abundant natural product available from sassafras oil in Brazil, as starting material [36,37]. This anti-inflammatory drug functions by non-selective inhibition of COX-1 and COX-2. Sulindac (**1**) is a pro-drug, containing a methyl sulfoxide group that is converted to the metabolites sulindac sulfide and sulindac sulfone in vivo (Fig. 1, **9**–**10**) [38]. It has been reported that sulindac sulfide, and not sulindac sulfone, blocks prostaglandin synthesis [39]. In addition, sulindac and its metabolites have been shown to play important roles in the prevention of colonic carcinogenesis [40–42] and may function as anti-apoptotic agents [29,43].

Based on the recent renewed interest in sulindac and its metabolites [40], our group designed and synthesized a new series of analogues of this classic NSAID, exploring the spatial similarities with selective NSAIDs of the diarylheterocyclic class, like celecoxib and rofecoxib (Fig. 1, **5**–**6**). The design concept is disclosed in Fig. 3.

These new sulindac analogues (**17a**–**i**) were planned by the substitution of the principal pharmacophoric group for COX-1 inhibitor activity, represented by the carboxylic acid moiety (A, Fig. 3), by different neutral amide residues (C, Fig. 3). Otherwise, in order to accomplish a better COX-1/COX-2 selectivity ratio for these new series of active compounds (**17a**–**i**), the introduction of the pharmacophoric methyl sulfone unit (D, Fig. 3), characteristic of several COX-2 selective inhibitors, such as rofecoxib (**6**), was planned in replacement for the methyl sulfoxide group (**B**, Fig. 3) present in the prototype **1**.

The designed compounds (**17a**–**i**) were synthesized using sulindac (**1**), a known marketed drug, as starting material and have been submitted to flexible docking studies using the X-ray crystallographic structure of COX-1 and COX-2 [44–48] and FlexE software [49] in order to build structure–activity relationship considerations. Finally, Lipinski's rule of five has been applied with

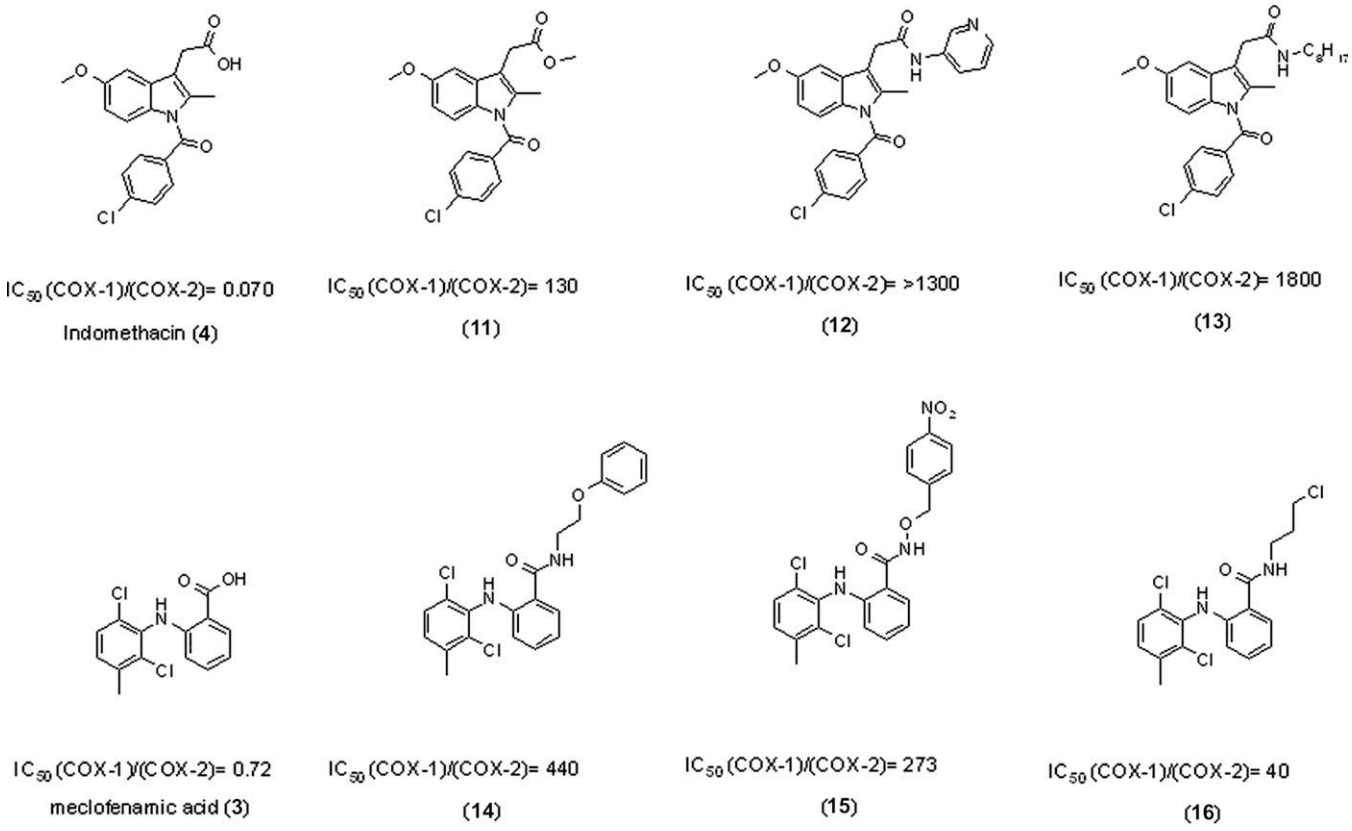

Fig. 2. Modified NSAIDs with better COX-1/COX-2 selectivity ratio.

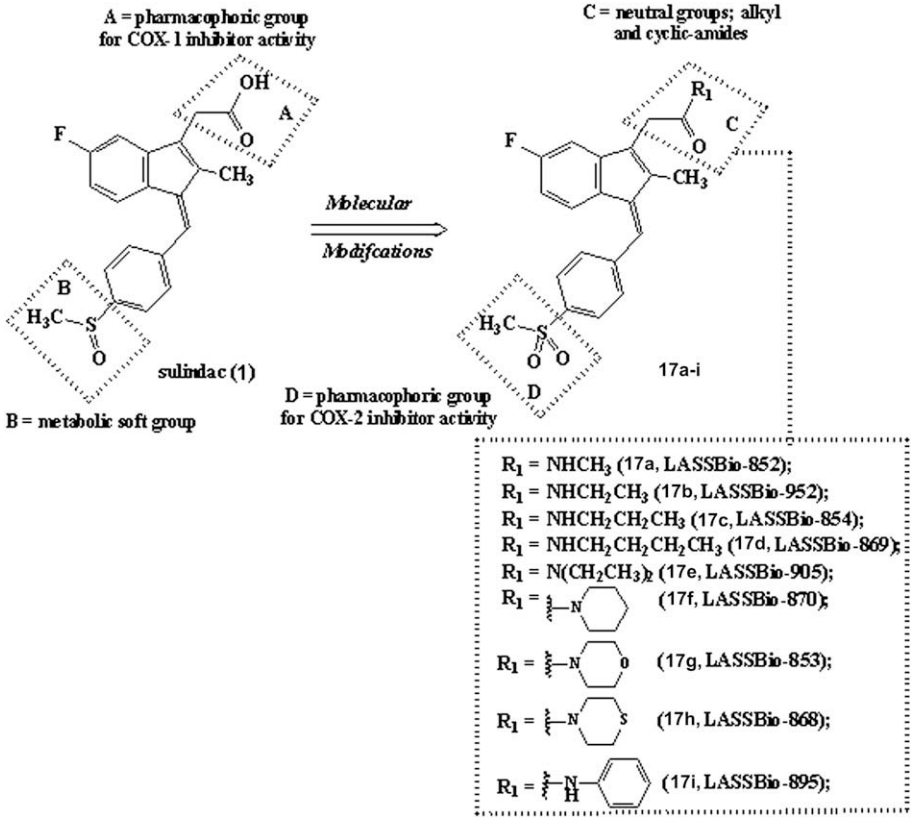

Fig. 3. Design concept of sulindac analogues, aimed at a better COX-1/COX-2 selectivity ratio.

the aim to predict cell permeability behavior of the new sulindac analogues (**17a**–**i**) [50]. The compounds were also evaluated for anti-inflammatory and antinociceptive activities in vivo.

2. Results and discussion

2.1. Synthesis

The synthesis of compounds (**17a**–**i**) was performed in three overall steps, using sulindac (**1**) as starting material (Scheme 1). In the synthetic approach compound methyl 2-5-fluoro-2-methyl-1-[1-(4-methylsulfonylphenyl)-(*Z*)-methylidene]-1*H*-3-indenylacetate (**19**) was identified as the key precursor. This compound was obtained in ca. 85% overall yield from sulindac, exploring the oxidation of methyl sulfoxide group and the esterification of the carboxylic acid group (Scheme 1) [51].

With an attractive method for access to the key intermediate (**19**), we next performed the condensation of this compound with functionalized alkyl and aryl amines, using aluminum chloride in dichloromethane boiled at reflux, under nitrogen atmosphere [52], to afford the corresponding sulfone-amides derivatives **17b**–**i** in moderate to excellent yields (Scheme 1). The methyl amide derivative (**17a**) was obtained in satisfactory yield by aminolysis of ester (**19**), using aqueous solution of methylamine 40% [53].

The methyl amide-sufoxide derivative (**20**) was obtained in two reaction steps, in 50% overall yield, exploring the esterification of carboxylic acid group of sulindac (**1**), followed by aminolysis of the corresponding ester using aqueous methylamine 40% (Scheme 1).

2.2. Biological assays

The antinociceptive and anti-inflammatory activities of the new sulindac analogues (**17a**–**i**, Fig. 3) were evaluated using the acetic acid induced mice abdominal constrictions test and the carrageenan-induced rat paw edema test, respectively [54]. All compounds and sulindac, used as positive control, were administered by oral administration at a screening dose of 300 μmol/kg and also evaluated for its ulcerogenic potential [55]. The results are disclosed in Tables 1 and 2.

The results demonstrated that all compounds showed antinociceptive activity in the tested dose (Table 1). The most potent antinociceptive derivatives were **17b** (LASSBio-952) and **17a** (LASSBio-852), bearing an ethyl amide and methyl amide side chain, respectively, with 59.4% and 43.4% of inhibition of the induced abdominal constrictions. The results obtained with the homologous **17c** (LASSBio-854, 38.6%) and **17d** (LASSBio-869, 34.6%), with amide side-chains of three and four carbon atoms, respectively, suggest some steric limitation in the putative bioreceptor (Table 1). This assumption is further corroborated by the low activity found for derivative **17e** (LASSBio-905, 13.9%), which has a bulky diethyl amide side chain. Aromatic amide side-chains are also not tolerated due to the low antinociceptive activity demonstrated by compound **17i** (LASSBio-895, 18.9%). As expected, derivative **20** (LASSBio-906, Scheme 1), synthesized in order to attribute the importance of the methyl sulfone subunit introduced in the structural design of this new bioactive series, which bears a methyl amide side chain and the methyl sulfoxide group, showed the lowest antinociceptive effect (6.3%) (Table 1), confirming the pharmacophoric profile of the methyl sulfone group for the antinociceptive activity.

The application of non-classic bioisosteric strategy [56] resulted in the design of compound **17f** (LASSBio-870) with significant analgesic activity (35.6%, Table 1). Subsequent bioisosteric replacement of methylene in the piperidine moiety of compound **17f** by oxygen or by sulfur atom result in the structural design of compounds **17g** (LASSBio-853) and **17h** (LASSBio-868), bearing a morpholine and thiomorpholine amide subunit, respectively. As depicted in Table 1, derivative **17h** (LASSBio-868) showed 47.8% of inhibition of the induced constrictions, close to the value observed for the prototype sulindac, 49%. Celecoxib, a selective COX-2 inhibitor, showed a superior inhibition of the constrictions by 55.6% (Table 1).

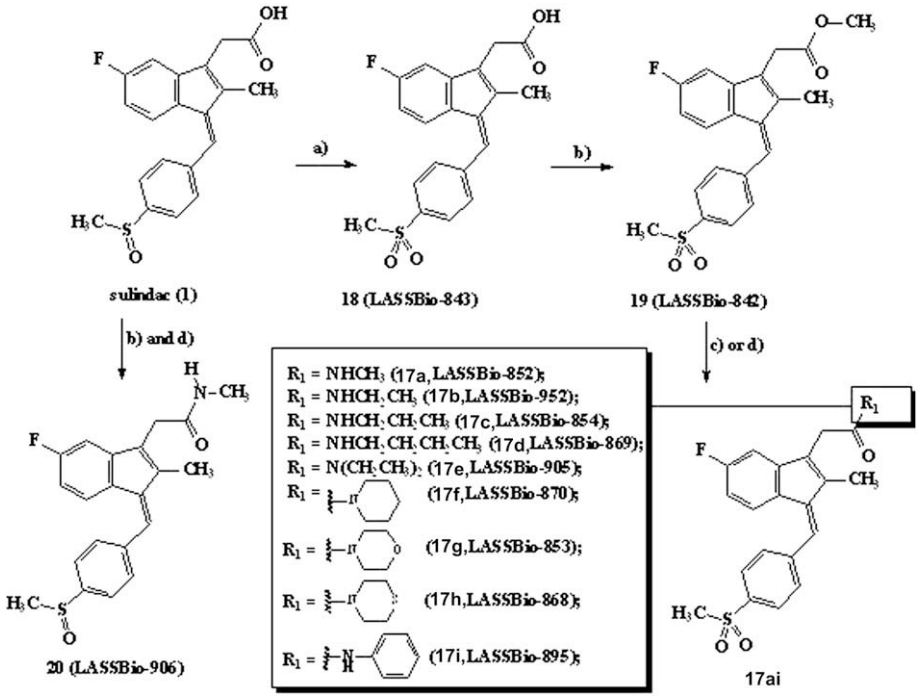

Scheme 1. Conditions: (a) Oxone®, THF:MeOH:H_2O, r.t., 1 h, 90%; (b) MeOH, H_2SO_4 cat., reflux, 1 h, 95%; (c) 1: $AlCl_3$, CH_2Cl_2, N_2, r.t.; 2: functionalized amines, CH_2Cl_2, reflux, 24 h, 50–94%; (d) aqueous methylamine 40%, 50 °C, 72 h, 45–50%.

Table 1
Effect of sulindac analogues on the inhibition of abdominal constrictions induced by acetic acid (0.1 N, i.p.) in mice.

Compound	Constrictions count	% Inhibition
Vehicle control (Arabic gum 5%)	60.6 ± 1.2	–
Sulindac	30.9 ± 2.1*	49%
Celecoxib	26.7 ± 1.7*	56%
17a	34.3 ± 2.8*	43%
17b	24.6 ± 2.4*	59%
17c	37.2 ± 1.8*	39%
17d	39.6 ± 3.8*	35%
17e	52.6 ± 3.8	14%
17f	39.0 ± 2.2*	36%
17g	46.5 ± 3.1*	22%
17h	31.6 ± 2.7*	48%
17i	49.5 ± 3.5	19%
18	39.8 ± 1.3*	34%
19	47.7 ± 1.5*	21%
20	57.2 ± 2.2	6%

All test compounds were administered at a dose of 300 μmol/kg p.o. $N = 8–10$ animals. Results are expressed as mean ± SEM. % of inhibition obtained by comparison with vehicle control group.
*$p > 0.05$ (Student's t-test).

Curiously, the sulindac sulfone acid derivative **18** (LASSBio-843), described as an inactive metabolite of sulindac (**1**), showed similar analgesic activity to compounds **17d** (LASSBio-869) and **17f** (LASSBio-870) with an inhibition of 34.3%. Finally, compound **19** (LASSBio-842), an synthetic intermediate, that bears a methyl ester side chain, was also evaluated and showed low antinociceptive activity, inhibiting the abdominal constrictions in only 21.2% (Table 1).

The results for the anti-inflammatory activity of sulindac analogues (**17a–i**), administered p.o. at a dose of 300 μmol/kg (Table 2), indicated that the most active compounds were sulindac (**1**), sulindac sulfone (**18**, LASSBio-843) and **17a** (LASSBio-852), that inhibited edema formation in 67%, 48% and 35%, respectively. According to what was expected, sulindac exerted a significant ulcerative behavior in the gastric mucosa in the carrageenan-induced rat paw edema assay (ulcerogenic potential = 2.0) supporting its non-selective COX mechanism of action. However, **18** (LASSBio-843, sulindac sulfone) and **17a** (LASSBio-852) had a lower or null ulcerogenic potential (0.4) (Table 2), probably because it bears a pharmacophoric methyl sulfone group, present in a variety of COX-2 inhibitors [17,19]. Thus, we may hypothesize that **18** (LASSBio-843, sulindac sulfone) works through the inhibition of COX-1 and COX-2, in a dual fashion, with some selectivity towards COX-2, in opposition to what has been reported in the literature in an in vitro assay of cancer cell lines [39]. Nevertheless, the interference of **18** (LASSBio-843, sulindac sulfone) in other enzyme pathways related to the inflammatory response cannot be discarded [57].

Table 2
Effect of sulindac analogues on the inhibition of carrageenan-induced rat paws edema (1 mg/paw; i.p.).

Compound	Edema (μl)[a]	% Inhibition	Ulcerogenic potential
Vehicle control (Arabic gum 5%)	569 ± 45	–	–
Sulindac	190 ± 28*	67%	2
Celecoxib	370 ± 27*	35%	0
17a	370 ± 37*	35%	0
17b	411 ± 54*	27%	0
17c	414 ± 27*	20%	1.4
17d	531 ± 11	7%	2
17e	415 ± 19*	27%	1.0
17f	461 ± 9*	19%	0
17g	546 ± 57	4%	0
17h	503 ± 22	11%	4
17i	497 ± 48	12%	0
18	299 ± 28*	48%	0.4
19	484 ± 34	15%	0
20	406 ± 32*	28%	0

All test compounds were administered at a dose of 300 μmol/kg p.o. $N = 8–10$ animals.
*$p > 0.05$ (Student's t-test).
[a] Edema was calculated as volume difference between carrageenan- and saline-treated paws after 3 h of carrageenan injection. Results are expressed as mean ± SEM. % of inhibition obtained by comparison with the vehicle control group.

Compound **17a** (LASSBio-852), bearing a methyl amide subunit, showed reasonable anti-inflammatory activity, in addition to the already mentioned good antinociceptive profile, inhibiting edema formation in 35%. The sulfoxide derivative of **17a**, compound **20** (LASSBio-906), showed an anti-inflammatory activity at the same magnitude of the former, inhibiting edema formation in 28%, however without showing an antinociceptive effect.

Furthermore, analogues bearing bulky or hydrophobic aromatic amides in the side-chains, such as **17b** (LASSBio-952), **17c** (LASSBio-854), **17d** (LASSBio-869), **17e** (LASSBio-905), **17f** (LASSBio-870), **17g** (LASSBio-853), **17h** (LASSBio-868) and **17i** (LASSBio-895), did not present good anti-inflammatory profiles, inhibiting edema formation very poorly (Table 2). These compounds showed a better antinociceptive profile than anti-inflammatory one. Surprisingly, compound **17h** (LASSBio-868), that bears a thiomorpholine group in its side chain, and was one of the most active compounds in the antinociceptive test, showed no significant anti-inflammatory activity.

We may hypothesize that this result is due to some sort of steric blockade exerted by this group on its biomolecular target. Finally, another curious result was the low anti-inflammatory activity of **19** (LASSBio-842), the methyl ester analogue, which is expected to be transformed, in vivo, into its carboxylic acid metabolite **18** (LASSBio-843, sulindac sulfone) (Table 2). As has been hypothesized in the analysis of the antinociceptive results (Table 1), it is possible that the time window in which the biological experiments have been performed was not wide enough to allow full biotransformation of this compound.

2.3. Molecular modeling

2.3.1. Molecular docking with COX-1 and COX-2

In an attempt to further corroborate the design strategy of the new sulindac analogues (**17a–i**), aimed at a better COX-1/COX-2 selectivity ratio, and try to establish the structure–activity relationship of the designed compounds, we performed flexible docking studies using available X-ray crystal structures of COX-1/COX-2 with bound inhibitors [44–48]. This theoretical study was performed using the software FlexE [49] with protein ensembles of both enzymes under study [44–48]. The proposed interaction modes of the ligands into the active site of COX-1 and COX-2 were determined as the highest scored conformations (best-fit ligand) among 30 conformational and binding modes generated according to FlexX scoring function, which corresponds to the structure with the most favorable free energy of binding, i.e. ΔG_{bind} (kJ/mol) (Fig. 4). ΔG values shown in this study have been based on PM3 charges [58] due to a better correlation between binding energy (ΔG_{bind}) and COX inhibition. Fig. 4 demonstrates that FlexE was able to predict the non-selective COX profile of sulindac sulfide (**9**) and the selective COX-2 profile of celecoxib (**5**) (Fig. 1).

In the analysis of the docked complexes, we have tried to get some qualitative assessment on the molecular basis of the biological activity of closely related compounds in our series, trying to correlate the biological data to the molecular design, keeping in mind that the assays have been performed in vivo, increasing the complexity of the biological response and, thus, of correlation to theoretical data. Only the best docking scores have been considered in this analysis (Figs. 5–8).

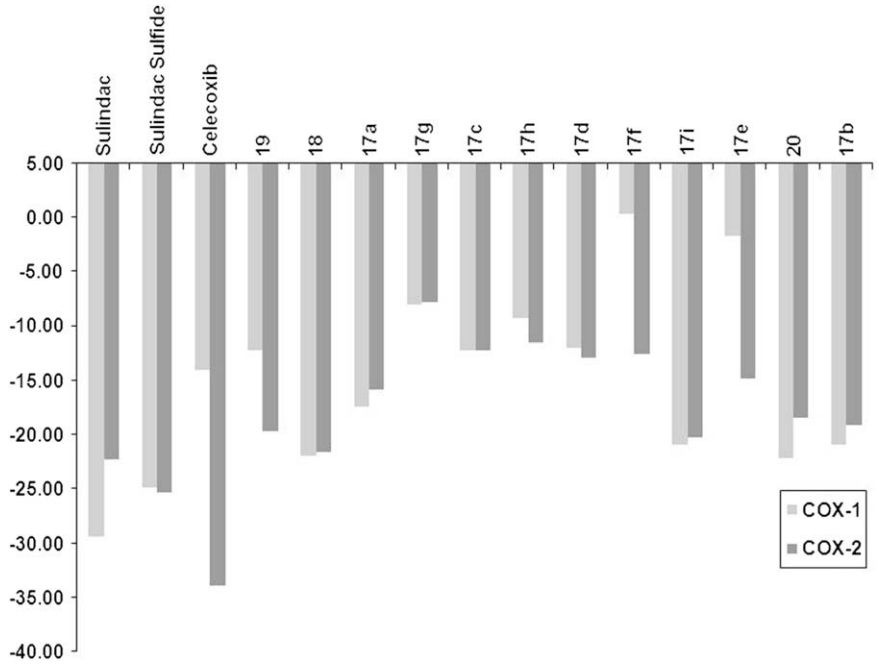

Fig. 4. Binding energies (ΔG_{bind}, kJ/mol) of top scoring solutions of the sulindac analogues as resulting from docking experiments.

Visual inspection of the obtained COX-1 complex with sulindac using flexible docking (Fig. 5a) reveals a binding pose in which the carboxylate group forms hydrogen bonds at the mouth of the cyclooxygenase active site, with Arg120 and Tyr355; the oxygen atom of the sulfoxide group forms a hydrogen bond with Ser530 and hydrophobic residues, such as Val349, Leu359 and Leu531 surround the phenyl–ethynyl group, within van der Waals contact distance. The same interactions involving the phenyl–ethynyl group can be seen for sulindac sulfide (Fig. 5b). Additionally, the methyl-sulfide group is close to the side chain of Met522 (Fig. 5b), performing hydrophobic interactions.

The obtained COX-2 complex with sulindac (Fig. 5c) reveals a binding pose in which this compound hydrogen bonds to Arg120 via its carboxylate group. Additional hydrophobic interactions involve Ala527, Leu531 and Leu534 (Fig. 5c). Furthermore, sulindac sulfide also interacts with Arg513 and Tyr355 via its carboxylate group (Fig. 5d) and is surrounded by Ile345, Met522, Val523 and Leu531, in close hydrophobic contacts. This result is in agreement with previous docking studies of this compound [59].

Compound **18** (LASSBio-843, sulindac sulfone) complexed with COX-1 (Fig. 6a) reveals an interesting binding mode in which the sulfone group, instead of the carboxylate group, forms hydrogen bonds with Arg120 and Tyr355. The carboxylate group hydrogen bonds to Ser530, close to the aromatic pocket comprised by Phe381, Tyr385 and Trp387 (Fig. 6a).

The visual inspection of the complex of **18** (LASSBio-843, sulindac sulfone) and COX-2 (Fig. 6b) reveals the same binding orientation that had been observed in COX-1, involving hydrogen bonding interactions of the oxygen atoms of the sulfone group at the mouth of the binding channel with Arg513 and His90. Furthermore, Val349, Phe518 and Leu531 are within van der Waals contact. Additional hydrogen bonds are observed between the oxygen atoms of the carboxylate group and the hydroxyl groups of Tyr385 and Ser530 (Fig. 6b). This result is in agreement to the observed binding modes for arachidonic acid and diclofenac with COX-2 in which their carboxylate groups are hydrogen-bonded to Tyr385 and Ser530, leading to enzyme inactivity [44,60]. These works demonstrate that the carboxylate group of an acidic non-steroidal anti-inflammatory drug can bind to a COX enzyme in an orientation that precludes the formation of a salt bridge with Arg120. Experiments of mutations suggested that Ser530 is also important in time-dependent inhibition by nimesulide and piroxicam [44].

Structure–activity relationship analysis of **17a** (LASSBio-852), **17b** (LASSBio-952), **17c** (LASSBio-854) and **17d** (LASSBio-869), that possess one, two, three, four carbon atoms in their side-chains, respectively, indicates that the amide side chain plays an important role in their interactions with COX-1, since these compounds show similar antinociceptive profiles (Table 1), although the ethyl amide side chain of **17b** (LASSBio-952) seems to be ideal for a better interaction with the bioreceptor, since this compound showed 59.4% of inhibition of abdominal constrictions induced by acetic acid (Table 1). Interestingly, the increasing, and therefore less favorable, ΔG_{bind} values observed in the docking results for COX-2 (Fig. 4) correlate well with the decreasing anti-inflammatory activity observed in the carrageenan-induced rat paw edema assay and with the increasing ulcerogenic action observed for these compounds, supporting the better anti-inflammatory profile observed for **17a** (LASSBio-852) in COX-2 pathway due to the absence of gastric ulcerogenicity (Table 2).

Fig. 7 discloses the interactions of **17d** (LASSBio-869) and **17b** (LASSBio-952) with COX-1 and COX-2. Compound **17d** (LASSBio-869) forms hydrogen bonds with COX-1 via one of the oxygen atoms of the sulfone group with Arg120 (Fig. 7a). A few hydrophobic contacts have been observed, involving Ile345, Val349, Leu359 and Leu531. Compound **17b** (LASSBio-952), that was very active in the anti-nociceptive bioassay, interacts with COX-1 in an inverted mode as compared to **17d** (LASSBio-869), hydrogen bonding with Arg120 and Tyr355 through its amide group (Fig. 7b). An additional hydrogen bonding interaction is observed between one of the oxygen atoms of its sulfone group and Trp387. Finally, hydrophobic contacts are observed involving Val116, Leu359, Ala527 and Leu531 (Fig. 7b).

The main interactions observed for **17d** (LASSBio-869) and COX-2 are hydrogen bonds involving the amide group, Arg120 and Tyr355, in an inverted binding mode (Fig. 7c). Further hydrophobic interactions are observed with Leu531 and Leu534 (Fig. 7c).

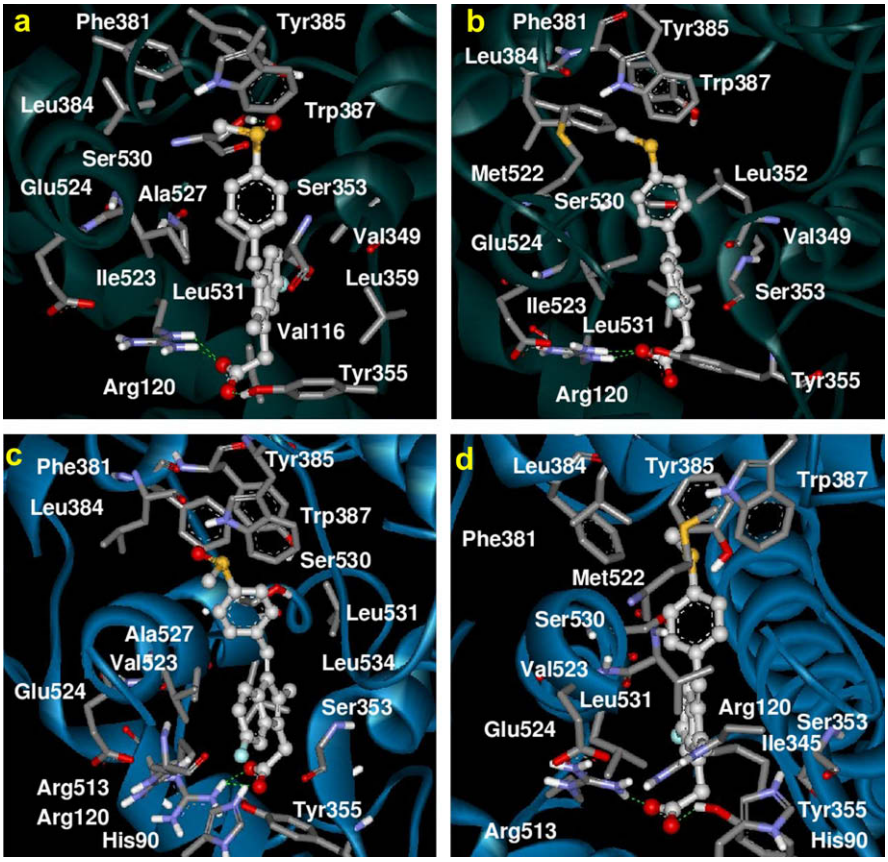

Fig. 5. Residues involved in the interactions with sulindac (a) and sulindac sulfide (b), in the binding site of COX-1 and in the binding site of COX-2 (c) and (d), respectively, as resulting from the top scored docking solutions obtained with FlexE. Hydrogen bonds are shown as green dashed lines. Only polar hydrogens are shown for clarity. (For interpretation of the references to color in this figure legend, the reader is referred to the web version of this article.)

However, it can be seen that the amide alkyl chain is protruding out of the entrance of the active site, probably due to steric clash with side-chains of amino acid residues in the binding site. Compound **17b** (LASSBio-952) interacts with COX-2 in the virtually same binding mode as with COX-1, hydrogen bonding with Arg120 and Tyr355 through the oxygen atom of the amide group (Fig. 7d) and with Trp387 through one of the oxygen atoms of its sulfone group. Only one hydrophobic contact has been observed, involving Val116. This lack of additional hydrophobic contacts may be an explanation for the low activity of this compound in the inflammation bioassay.

Despite the lack of correlation of experimental biological activities with ΔG_{bind}, the putative binding modes with COX-1 of **17h** (LASSBio-868), a thiomorpholine derivative which was the most active compound in the antinociceptive assay and **17g** (LASSBio-853), a morpholine derivative, one the less active (Table 1), have been investigated (Fig. 8). Analysis of the complex of **17g** (LASSBio-853) in its best docked position with COX-1 (Fig. 8a) reveals hydrogen bonds of the former involving the oxygen atom of the amide carbonyl with Arg120 and one of the oxygen atoms of the sulfone group with Tyr385. Also, the $2CH_3$ group in the indene

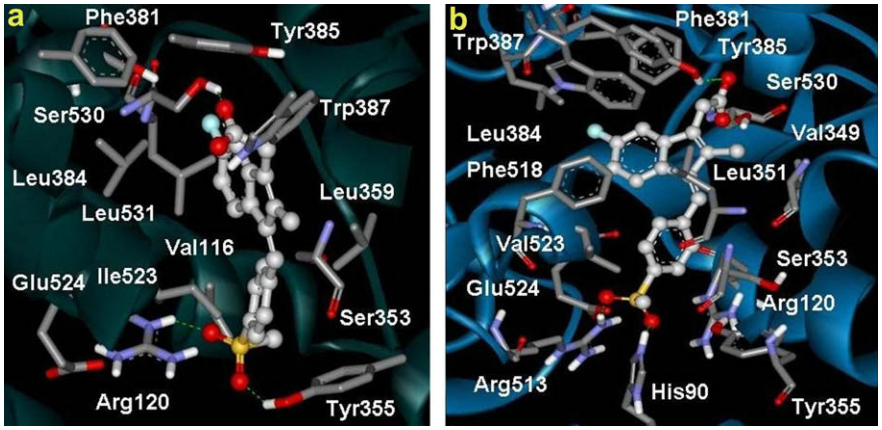

Fig. 6. Residues involved in the interactions with **18** (LASSBio-843, sulindac sulfone) in the binding site of COX-1 (a) and COX-2 (b) as resulting from the top scored docking solutions obtained with FlexE. Hydrogen bonds are shown as green dashed lines. Only polar hydrogens are shown for clarity. (For interpretation of the references to color in this figure legend, the reader is referred to the web version of this article.)

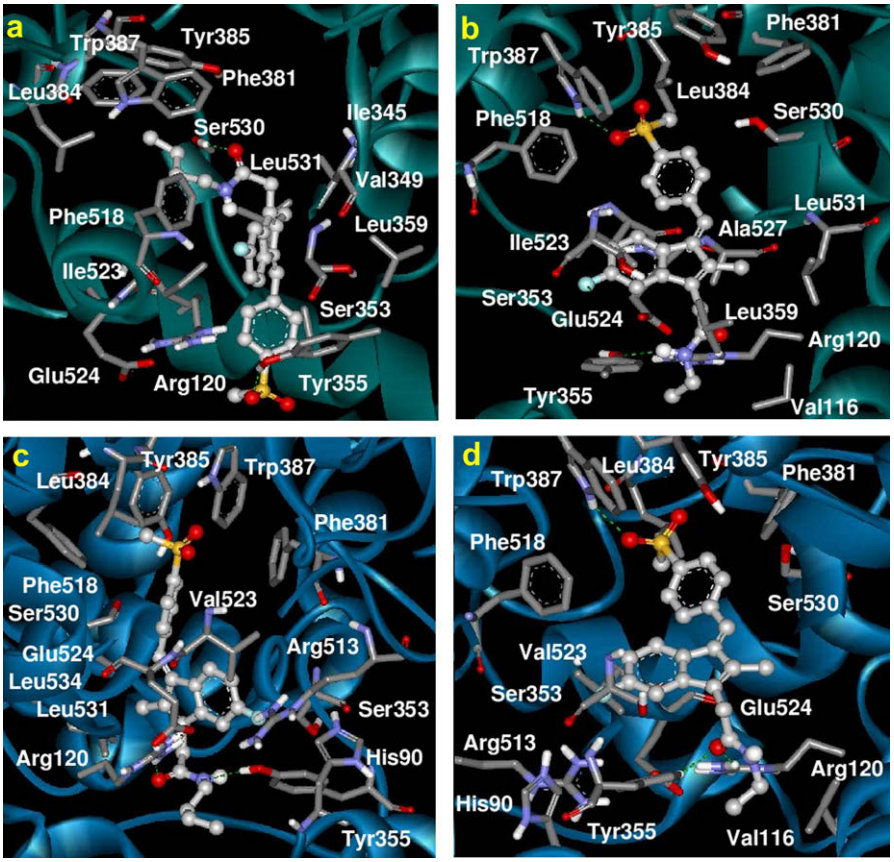

Fig. 7. Residues involved in the interactions with **17d** (LASSBio-869) (a) and **17b** (LASSBio-952) (b) in the binding site of COX-1 and in the binding site of COX-2 (c) and (d), respectively, as resulting from the top scored docking solutions obtained with FlexE. Hydrogen bonds are shown as green dashed lines. Only polar hydrogens are shown for clarity. (For interpretation of the references to color in this figure legend, the reader is referred to the web version of this article.)

system is in close van der Waals contact with Leu359 while the fluorine atom is close to Ile523 and the morpholine ring is in van der Waals contact with Val116 (Fig. 8a). However, the best docked position of LASSBio-868 with COX-1 (Fig. 8b) shows an inversed binding orientation compared to **17g** (LASSBio-853). Finally, one of the oxygen atoms of the sulfone moiety hydrogen bonds to Tyr355 at the mouth of the channel and the oxygen atom of the amide side chain forms hydrogen bonds with Ser530 (Fig. 8b).

2.3.2. *Lipinski's rule of five*

The bioavailability of compounds **17a–i** was assessed using ADME (absorption, distribution, metabolism, elimination) prediction methods. In particular, we calculated the compliance of compounds to the Lipinski's rule of five [50]. Briefly, this simple rule is based on the observation that most orally administered drugs have a molecular weight (MW) of 500 or less, a log *P* not higher than 5, five or fewer hydrogen bond donor sites and 10 or fewer hydrogen bond

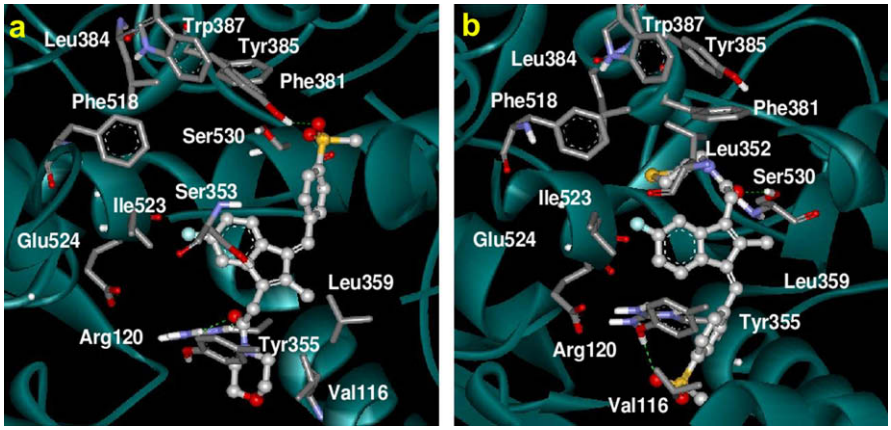

Fig. 8. Residues involved in the interactions with **17g** (LASSBio-853) (a) and **17h** (LASSBio-868) (b) in the binding site of COX-1, as resulting from the top scored docking solutions obtained with FlexE. Hydrogen bonds are shown as green dashed lines. Only polar hydrogens are shown for clarity. (For interpretation of the references to color in this figure legend, the reader is referred to the web version of this article.)

Table 3
Compliance of the sulindac analogues to computational parameters of bioavailability.

Compounds	CLOGP[a]	Molecular weight (MW)	Number of hydrogen bonding acceptors	Number of hydrogen bonding donors	PSA[b]
Sulindac	3.16	355.405	3	1	125.46
Sulindac sulfide	5.31	339.406	2	1	105.45
Celecoxib	4.37	381.374	4	1	145.01
17a	2.22	385.454	3	1	105.96
17b	2.75	399.481	3	1	110.20
17c	3.28	413.508	3	1	102.04
17d	3.81	427.534	3	1	94.85
17e	3.56	427.534	3	–	82.62
17f	3.28	439.545	3	–	85.92
17g	2.49	441.518	4	–	102.15
17h	3.22	457.584	3	–	112.24
17i	4.46	447.524	3	1	96.23
18	2.86	371.404	4	1	143.40
19	3.48	386.439	4	–	119.25
20	2.27	369.4548	2	1	85.72

[a] Calculated octanol/water coefficient [63].
[b] Polar Surface Area, calculated as the surface area of all O/N/S atoms and hydrogens covalently bonded to these atoms.

acceptor sites (N and O atoms). In addition, we calculated the polar surface area (PSA) since it is another key property that has been linked to drug bioavailability. Thus, passively absorbed molecules with a PSA > 140 Å^2 are thought to have low oral bioavailability [61]. The results disclosed in Table 3 show that all synthesized compounds comply with these rules, except for celecoxib and sulindac sulfone, that violate only one parameter, PSA. Theoretically, these compounds should present good passive oral absorption and differences in their bioactivity cannot be attributed to this property.

3. Conclusions

The results described in this work show that all of the sulindac analogues have significant antinociceptive activity, measured by the inhibition of abdominal constrictions induced by acetic acid. The most active compounds were **17b** (LASSBio-952), which has an ethyl amide side chain; **17a** (LASSBio-852), which presents a methyl amide side chain and **17h** (LASSBio-868) that presents the thiomorpholine amide ring in its side chain.

The anti-inflammatory assay, measured by inhibition of carrageenan-induced rat paw edema, showed that **18** (LASSBio-843), the sulfone metabolite of sulindac, was the most active compound, followed by **17a** (LASSBio-852), confirming these compounds as potential inhibitors of COX enzymes, without significant gastric ulcerogenic effects, as compared to sulindac.

Molecular modeling studies with COX-1 and COX-2 revealed an "inversed" orientation in the putative binding mode of **18** (LASSBio-843), which presents special hydrogen bonding interactions with amino acid residues of COX-2, like Tyr385 and Ser530, as already reported for other known NSAIDs [44,45,60]. Although reports in the literature discard the direct COX activity of this compound, the results reported herein suggest modulation of the prostaglandin pathway that may either be dependent or independent of COX activity [57]. Finally, according to Lipinski's rule of five, the synthesized compounds should present good oral absorption.

4. Experimental

Melting points were determined with a Quimis 340 apparatus and are uncorrected. ^{1}H NMR spectra, unless otherwise stated, were obtained in deuterated dimethylsulfoxide or deuterated chloroform containing ca. 1% tetramethylsilane as an internal standard using a Bruker AC 200 spectrometer at 200 MHz. Splitting patterns are as follows: s, singlet; d, doublet; dd, double doublet; dt, triple doublet; q, quartet; br, broad; m, multiplet. ^{13}C NMR spectra were obtained using the same spectrometer described above at 50 MHz, using deuterated dimethylsulfoxide or deuterated chloroform as internal standard. Microanalysis data were obtained using a Perkin–Elmer 240 analyser, using a Perkin–Elmer AD-4 balance. The progress of all reactions was monitored by TLC performed on 2.0 × 6.0 cm aluminium sheets precoated with silica gel 60 (HF-254, E. Merck) to a thickness of 0.25 mm. The developed chromatograms were viewed under ultraviolet light at 254 nm. E. Merck silica gel (60–200 mesh) was used for column chromatography.

4.1. Synthesis

4.1.1. 2-((1Z)-1-(4-(Methylsulfonyl)benzylidene)-5-fluoro-2-methyl-1-H-inden-3-yl)acetic acid (**18**)

To a solution of 1 mmol of sulindac (**1**) in 12 mL of THF, 4 mL of MeOH and 4 mL of H_2O, at 0 °C, was added 5 mmol of potassium hydrogen persulfate (Oxone®). The reaction mixture was stirred for 1 h at room temperature, when the end of reaction was observed by TLC. The suspension was evaporated to half of its original, followed by addition of 50 mL of cold water to result in the formation of a yellow precipitate, which was filtered, washed with water and dried under reduced pressure to give sulfone derivative (**18**) in 90% of yield, mp = 194–196 °C.

NMR ^{1}H (200 MHz, DMSO d_6) δ: 2.16 (s, ArC*H*$_3$); 3.28 (s, SO_2CH_3); 3.57 (s, ArCH_2CO_2H); 6.71 (td, J = 8.4 Hz, 9.5 Hz and 2.5 Hz, H6); 7.02 (dd, J = 9.5 Hz and 2.5 Hz, H4); 7.12 (dd, J = 5.2 Hz and 8.4 Hz, H7); 7.36 (s, C=C*H*); 7.78 (d, J = 8.2 Hz, H2' and H6′); 8.00 (d, J = 8.2 Hz, H3′ and H5′) ppm.

Anal. Calcd. for $C_{20}H_{17}O_4SF$: C, 64.50; H, 4.60. Found: C, 64.49; H, 4.59.

4.1.2. Methyl 2-((1Z)-1-(4-(methylsulfonyl)benzylidene)-5-fluoro-2-methyl-1-H-inden-3-yl)acetate (**19**)

To a carboxylic acid derivative (1 mmol) were added methanol (20 mL) and catalytic amounts of H_2SO_4. The mixture was refluxed for 1 h under a water separator (Dean–Stark apparatus). The reaction was stopped and the solvent was removed under reduced pressure. The total product mixture was dissolved in dichloromethane treated with NaOH 10% and washed with water. The organic layer was dried (Na_2SO_4), filtered and evaporated under reduced pressure to give desired ester derivative in 95% of yield, mp = 169–171 °C.

NMR ^{1}H (200 MHz, $CDCl_3$) δ: 2.20 (s, ArC*H*$_3$); 3.14 (s, SO_2CH_3); 3.57 (s, ArCH_2CO_2H); 3.71 (s, CO_2CH_3); 6.56 (td, J = 8.4 Hz, 9.5 Hz and 2.5 Hz, H6); 6.88 (dd, J = 9.5 Hz and 2.5 Hz, H4); 7.10 (dd, J = 5.1 Hz and 8.4 Hz, H7); 7.12 (s, C=C*H*); 7.70 (d, J = 8.0 Hz, H2′ and H6′); 8.00 (d, J = 8.0 Hz, H3′ and H5′) ppm.

NMR ^{13}C (50 Hz, $CDCl_3$) δ: 10.7 (Ar*C*H$_3$); 31.7 (ArCH_2CO_2R); 44.7 (SO_2CH_3); 52.5 (ArCO_2CH_3); 106.5 (C4); 110.9 (C6); 123.8 (C7); 127.4 (C=*C*H); 127.6 (C2′ and C6′); 129.5 (C2); 130.4 (C3′ and C5′); 132.4 (C1′); 138.3 (C3); 140.0 (C4′); 142.6 (C7a); 147.0 (C3a); 161.2 (C1); 166.1 (C5); 170.8 (Ar*C*O_2R) ppm.

Anal. Calcd. for $C_{21}H_{19}O_4SF$: C, 65.27; H, 4.96. Found: C, 65.29; H, 4.99.

4.1.3. General procedure for the preparation of 2-5-fluoro-2-methyl-1-[1-(4-methylsulfonylphenyl)-(Z)-methylidene]-1H-3-indenyl amide derivatives (**17b–i**)

Aluminium chloride (10 mmol) was suspended at room temperature in dry dichloromethane (20 mL) under nitrogen atmosphere. The amine (10 mmol) was added dropwise, resulting in a colorless solution. After 10 min, a solution of the ester derivative (1 mmol) in dry dichloromethane (10 mL) was, carefully,

added. The reaction mixture was stirred for 24 h at reflux, when the end of reaction was observed by TLC. After that, the reaction mixture was diluted with 50 mL of dichloromethane and extracted with aqueous HCl 10% (5 × 25 mL). The organic layer was dried over anhydrous sodium sulfate, filtered and evaporated under reduced pressure to furnish the amines derivatives (**17b–i**) in good to excellent yields. Compounds **17b–i** were purified by recrystallization in ethanol or in hydro-alcoholic mixture (1:1).

*4.1.3.1. 2-((1Z)-1-(4-(Methylsulfonyl)benzylidene)-5-fluoro-2-methyl-1-*H*-inden-3-yl)-*N*-ethylacetamide (**17b**).* Derivative **17b** was obtained as yellow crystals in 50% yield, mp 182–185 °C.

NMR ^{1}H (200 MHz, $CDCl_3$) δ: 1.18 (t, J = 7.2 Hz, $CONHCH_2CH_3$); 2.21 (s, $ArCH_3$); 3.15 (s, SO_2CH_3); 3.28 (q, J = 7.2 Hz, $CONHCH_2CH_3$); 3.51 (s, $ArCH_2CONHR$); 5.58 (br, CONH); 6.60 (td, J = 8.3 Hz, 9.2 Hz and 2.2 Hz, H6); 6.87 (dd, J = 9.2 Hz and 2.2 Hz, H4); 7.12 (dd, J = 4.9 Hz and 8.3 Hz, H7); 7.17 (s, C═CH); 7.72 (d, J = 8.1 Hz, H2′ and H6′); 8.02 (d, J = 8.1 Hz, H3′ and H5′) ppm.

Anal. Calcd. for $C_{22}H_{22}O_3NSF$: C, 66.15; H, 5.55; N, 3.51. Found: C, 66.14; H, 5.55; N, 3.49.

*4.1.3.2. 2-((1Z)-1-(4-(Methylsulfonyl)benzylidene)-5-fluoro-2-methyl-1-*H*-inden-3-yl)-*N*-propylacetamide (**17c**).* Derivative **17c** was obtained as yellow crystals in 92% yield, mp 182–184 °C.

NMR ^{1}H (200 MHz, $CDCl_3$) δ: 0.83 (t, J = 7.4 Hz, $CONHCH_2CH_2CH_3$); 1.46 (m, $CONHCH_2CH_2CH_3$); 2.21 (s, $ArCH_3$); 3.14 (s, SO_2CH_3); 3.17 (m, $CONHCH_2CH_2CH_3$); 3.51 (s, $ArCH_2CONHR$); 5.80 (br, CONH); 6.60 (td, J = 8.3 Hz, 9.2 Hz and 2.3 Hz, H6); 6.86 (dd, J = 9.2 Hz and 2.3 Hz, H4); 7.12 (dd, J = 5.1 Hz and 8.3 Hz, H7); 7.16 (s, C═CH); 7.71 (d, J = 8.1 Hz, H2′ and H6′); 8.01 (d, J = 8.1 Hz, H3′ and H5′) ppm.

NMR ^{13}C (50 Hz, $CDCl_3$) δ: 10.7 ($ArCH_3$); 11.3 ($CONHCH_2CH_2CH_3$); 22.9 ($CONHCH_2CH_2CH_3$); 33.9 ($ArCH_2CONHR$); 41.58 ($CONHCH_2CH_2CH_3$); 44.6 (SO_2CH_3); 106.4 (C4); 111.4 (C6); 123.9 (C7); 127.9 (C═CH, C2′ and C6′); 129.5 (C2); 130.3 (C3′ and C5′); 133.4 (C1′); 138.7 (C3); 140.2 (C4′); 142.4 (C7a); 146.7 (C3a); 161.2 (C1); 166.2 (C5); 169.1 (ArCONHR) ppm.

Anal. Calcd. for $C_{23}H_{24}O_3NSF$: C, 66.81; H, 5.85; N, 3.39. Found: C, 66.80; H, 5.86; N, 3.40.

*4.1.3.3. 2-((1Z)-1-(4-(Methylsulfonyl)benzylidene)-5-fluoro-2-methyl-1-*H*-inden-3-yl)-*N*-butylacetamide (**17d**).* Derivative **17d** was obtained as yellow crystals in 91% yield, mp 161–163 °C.

NMR ^{1}H (200 MHz, $CDCl_3$) δ: 0.87 (t, J = 7.0 Hz, $CONHCH_2CH_2CH_2CH_3$); 1.28 (m, $CONHCH_2CH_2CH_2CH_3$); 1.39 (m, $CONHCH_2CH_2CH_2CH_3$); 2.21 (s, $ArCH_3$); 3.14 (s, SO_2CH_3); 3.23 (q, J = 6.6 Hz, $CONHCH_2CH_2CH_2CH_3$); 3.51 (s, $ArCH_2CONHR$); 5.70 (br, CONH); 6.61 (td, J = 8.6 Hz, 9.0 Hz and 2.3 Hz, H6); 6.86 (dd, J = 9.0 Hz and 2.3 Hz, H4); 7.11 (dd, J = 5.2 Hz and 8.6 Hz, H7); 7.17 (s, C═CH); 7.71 (d, J = 8.0 Hz, H2′ and H6′); 8.02 (d, J = 8.0 Hz, H3′ and H5′) ppm.

NMR ^{13}C (50 Hz, $CDCl_3$) δ: 10.7 ($ArCH_3$); 13.8 ($CONHCH_2CH_2CH_2CH_3$); 20.1 ($CONHCH_2CH_2CH_2CH_3$); 31.7 ($CONHCH_2CH_2CH_2CH_3$); 33.9 ($ArCH_2CONHR$); 39.7 ($CONHCH_2CH_2CH_2CH_3$); 44.6 (SO_2CH_3); 106.4 (C4); 111.4 (C6); 124.0 (C7); 127.7 (C═CH, C2′ and C6′); 129.5 (C2); 130.3 (C3′ and C5′); 133.4 (C1′); 138.6 (C3); 140.2 (C4′); 142.4 (C7a); 146.7 (C3a); 161.2 (C1); 166.2 (C5); 169.0 (ArCONHR) ppm.

Anal. Calcd. for $C_{23}H_{24}O_3NSF$: C, 67.42; H, 6.13; N, 3.28. Found: C, 67.44; H, 6.15; N, 3.29.

*4.1.3.4. 2-((1Z)-1-(4-(Methylsulfonyl)benzylidene)-5-fluoro-2-methyl-1-*H*-inden-3-yl)-*N*-diethylacetamide (**17e**).* Derivative **17e** was obtained as yellow crystals in 75% yield, mp 68–70 °C.

NMR ^{1}H (200 MHz, $CDCl_3$) δ: 1.18 (m, $CON(CH_2CH_3)_2$); 2.17 (s, $ArCH_3$); 3.13 (s, SO_2CH_3); 3.4 (m, $CON(CH_2CH_3)_2$); 3.59 (s, $ArCH_2CONR_2$); 6.53 (td, J = 8.0 Hz, 9.2 Hz and 2.1 Hz, H6); 6.90 (dd, J = 9.2 Hz and 2.1 Hz, H4); 7.06 (dd, J = 5.1 Hz and 8.0 Hz, H7); 7.17 (s, C═CH); 7.68 (d, J = 8.1 Hz, H2′ and H6′); 7.99 (d, J = 8.1 Hz, H3′ and H5′) ppm.

NMR ^{13}C (50 Hz, $CDCl_3$) δ: 10.7 ($ArCH_3$); 13.2 and 14.4 ($CON(CH_2CH_3)_2$); 31.9 ($ArCH_2CONR_2$); 40.8 and 42.5 ($CON(CH_2CH_3)_2$); 44.7 (SO_2CH_3); 106.7 (C4); 110.9 (C6); 123.6 (C7); 126.6 (C═CH); 127.7 (C2′ and C6′); 129.5 (C2); 130.4 (C3′ and C5′); 134.2 (C1′); 136.6 (C3); 139.9 (C4′); 142.7 (C7a); 147.4 (C3a); 161.2 (C1); 166.1 (C5); 168.6 ($ArCONR_2$) ppm.

Anal. Calcd. for $C_{23}H_{24}O_3NSF$: C, 67.42; H, 6.13; N, 3.28. Found: C, 67.41; H, 6.13; N, 3.29.

*4.1.3.5. 2-((1Z)-1-(4-(Methylsulfonyl)benzylidene)-5-fluoro-2-methyl-1-*H*-inden-3-yl)-1-(piperidin-1-yl)ethanone (**17f**).* Derivative **17f** was obtained as yellow crystals in 82% yield, mp 196–198 °C.

NMR ^{1}H (200 MHz, $CDCl_3$) δ: 1.52 (m, $CON(CH_2)_2(CH_2)_3$); 2.17 (s, $ArCH_3$); 3.13 (s, SO_2CH_3); 3.45 (m, $CON(CH_2)_2(CH_2)_3$); 3.59 (s, $ArCH_2CONR_2$); 6.53 (td, J = 8.1 Hz, 9.2 Hz and 1.9 Hz, H6); 6.90 (dd, J = 9.2 Hz and 1.9 Hz, H4); 7.08 (dd, J = 5.1 Hz and 8.1 Hz, H7); 7.10 (s, C═CH); 7.69 (d, J = 8.2 Hz, H2′ and H6′); 7.99 (d, J = 8.1 Hz, H3′ and H5′) ppm.

NMR ^{13}C (50 Hz, $CDCl_3$) δ: 10.7 ($ArCH_3$); 24.6, 25.7 and 26.5 ($CON(CH_2)_2(CH_2)_3$); 31.9 ($ArCH_2CONR_2$); 43.3 and 47.2 ($CON(CH_2)_2(CH_2)_3$); 44.7 (SO_2CH_3); 106.7 (C4); 110.9 (C6); 123.6 (C7); 126.6 (C═CH); 127.7 (C2′ and C6′); 129.5 (C2); 130.4 (C3′ and C5′); 134.1 (C1′); 137.0 (C3); 139.9 (C4′); 142.7 (C7a); 147.3 (C3a); 161.2 (C1); 166.1 (C5); 167.8 ($ArCONR_2$) ppm.

Anal. Calcd. for $C_{25}H_{26}O_3NSF$: C, 68.32; H, 5.96; N, 3.19. Found: C, 68.31; H, 5.95; N, 3.22.

*4.1.3.6. 2-((1Z)-1-(4-(Methylsulfonyl)benzylidene)-5-fluoro-2-methyl-1-*H*-inden-3-yl)-1-morpholinoethanone (**17g**).* Derivative **17g** was obtained as yellow crystals in 90% yield, mp 198–201 °C.

NMR ^{1}H (200 MHz, $CDCl_3$) δ: 2.18 (s, $ArCH_3$); 3.14 (s, SO_2CH_3); 3.54 (m, $CON(CH_2)_2$); 3.60 (s, $ArCH_2CONR_2$); 3.67 (m, $O(CH_2)_2$); 6.62 (td, J = 8.1 Hz, 9.0 Hz and 2.0 Hz, H6); 6.89 (dd, J = 9.0 Hz and 2.0 Hz, H4); 7.09 (dd, J = 5.2 Hz and 8.1 Hz, H7); 7.11 (s, C═CH); 7.70 (d, J = 8.2 Hz, H2′ and H6′); 8.01 (d, J = 8.1 Hz, H3′ and H5″) ppm.

NMR ^{13}C (50 Hz, $CDCl_3$) δ: 10.8 ($ArCH_3$); 31.6 ($ArCH_2CONR_2$); 42.6 and 46.5 ($CON(CH_2)_2$); 44.7 (SO_2CH_3); 66.8 ($O(CH_2)_2$); 106.5 (C4); 111.1 (C6); 123.8 (C7); 127.0 (C═CH); 127.9 (C2″ and C6′); 129.5 (C2); 130.4 (C3′ and C5′); 133.3 (C1′); 136.0 (C3); 139.9 (C4′); 142.5 (C7a); 147.0 (C3a); 161.2 (C1); 166.1 (C5); 168.4 ($ArCONR_2$) ppm.

Anal. Calcd. for $C_{24}H_{24}O_4NSF$: C, 65.29; H, 5.48; N, 3.17. Found: C, 65.27; H, 5.49; N, 3.19.

*4.1.3.7. 2-((1Z)-1-(4-(Methylsulfonyl)benzylidene)-5-fluoro-2-methyl-1-*H*-inden-3-yl)-1-thiomorpholinoethanone (**17h**).* Derivative **17h** was obtained as yellow crystals in 71% yield, mp 196–198 °C.

NMR ^{1}H (200 MHz, $CDCl_3$) δ: 2.18 (s, $ArCH_3$); 2.56 (m, $S(CH_2)_2$); 3.13 (s, SO_2CH_3); 3.60 (s, $ArCH_2CONR_2$); 3.84 (m, $CON(CH_2)_2$); 6.56 (td, J = 8.1 Hz, 9.0 Hz and 2.1 Hz, H6); 6.91 (dd, J = 9.0 Hz and 2.1 Hz, H4); 7.09 (dd, J = 5.2 Hz and 8.1 Hz, H7); 7.11 (s, C═CH); 7.69 (d, J = 8.1 Hz, H2′ and H6′); 8.00 (d, J = 8.1 Hz, H3′ and H5′) ppm.

NMR ^{13}C (50 Hz, $CDCl_3$) δ: 10.8 ($ArCH_3$); 27.4 ($S(CH_2)_2$); 32.3 ($ArCH_2CONR_2$); 44.7 (SO_2CH_3); 44.9 and 48.9 ($CON(CH_2)_2$); 106.7 (C4); 111.1 (C6); 123.8 (C7); 127.0 (C═CH); 127.7 (C2′ and C6′); 129.5 (C2); 130.4 (C3′ and C5′); 133.3 (C1′); 137.5 (C3); 140.1 (C4′); 142.5 (C7a); 147.0 (C3a); 161.2 (C1); 166.1 (C5); 168.1 ($ArCONR_2$) ppm.

Anal. Calcd. for $C_{24}H_{24}O_3NS_2F$: C, 63.00; H, 5.29; N, 3.06. Found: C, 63.01; H, 5.29; N, 3.09.

*4.1.3.8. 2-((1Z)-1-(4-(Methylsulfonyl)benzylidene)-5-fluoro-2-methyl-1-*H*-inden-3-yl)-*N*-phenylacetamide (**17i**).* Derivative **17i** was obtained as yellow crystals in 94% yield, mp 220 °C (with decomposition).

NMR ^{1}H (200 MHz, DMSO d_6) δ: 2.22 (s, ArCH_3); 3.28 (s, SO_2CH_3); 3.68 (s, ArCH_2CONR$_2$); 6.71 (td, J = 8.0 Hz, 9.0 Hz and 2.2 Hz, H6); 7.04 (dd, J = 9.0 Hz and 2.2 Hz, H4); 7.09 (dd, J = 5.2 Hz and 8.0 Hz, H7); 7.11 (s, C=C*H*); 7.29 (m, H3″, H4″ and H5″); 7.59 (m, H2″ and H6″); 7.78 (d, J = 8.3 Hz, H2′ and H6′); 8.01 (d, J = 8.3 Hz, H3′ and H5′) ppm.

NMR ^{13}C (50 Hz, DMSO d_6) δ: 11.0 (Ar*C*H$_3$); 34.1 (Ar*C*H$_2$-CONHPh); 44.1 (SO_2CH_3); 107.2 (C4); 111.1 (C6); 119.8 (C2″ and C6″); 123.8 (C7); 124.0 (C4″); 127.5 (C=*C*H); 127.8 (C2′ and C6′); 129.3 (C3″ and C5″); 129.5 (C2); 130.6 (C3′ and C5′); 134.4 (C1′); 138.7 (C3); 139.7 (C4′); 140.8 (C1″); 142.2 (C7a); 147.9 (C3a); 160.9 (C1); 165.7 (C5); 168.4 (ArCONR$_2$) ppm.

Anal. Calcd. for $C_{26}H_{22}O_3NSF$: C, 69.78; H, 4.95; N, 3.13. Found: C, 69.79; H, 4.96; N, 3.15.

*4.1.4. 2-((1Z)-1-(4-(Methylsulfonyl)benzylidene)-5-fluoro-2-methyl-1-*H*-inden-3-yl)-*N*-methylacetamide (**17a**)*

Aminolysis was carried out by mixing ester **19** (1 mmol) with aqueous methylamine 40% (30 mmol). The reaction mixture was heated for 72 h at 50 °C. Then, it was cooled, added cold water (50 mL) and the resulting solid was collected and purified by column chromatography on silica gel (CH_2Cl_2 and CH_2Cl_2:MeOH 1%). Derivative **17a** was obtained as yellow crystals in 45% yield, mp 206–208 °C.

NMR ^{1}H (200 MHz, DMSO d_6) δ: 2.17 (s, ArCH_3); 2.58 (s, ArCONHCH_3); 3.28 (s, SO_2CH_3); 3.40 (s, ArCH_2CONHR); 5.80 (br, CON*H*); 6.70 (td, J = 8.3 Hz, 9.0 Hz and 2.1 Hz, H6); 6.95 (dd, J = 9.0 Hz and 2.1 Hz, H4); 7.13 (dd, J = 5.2 Hz and 8.3 Hz, H7); 7.33 (s, C=C*H*); 7.77 (d, J = 8.0 Hz, H2′ and H6′); 8.01 (d, J = 8.0 Hz, H3′ and H5′) ppm.

NMR ^{13}C (50 Hz, DMSO d_6) δ: 10.9 (Ar*C*H$_3$); 26.3 (CONHCH_3); 33.2 (Ar*C*H$_2$CONHCH_3); 43.9 (SO_2CH_3); 106.8 (C4); 110.8 (C6); 123.6 (C7); 128.9 (C=*C*H); 127.4 (C2′ and C6′); 129.8 (C2); 130.1 (C3′ and C5′); 134.6 (C1′); 138.2 (C3); 140.6 (C4′); 141.6 (C7a); 147.9 (C3a); 160.7 (C1); 165.6 (C5); 169.6 (Ar*C*ONHCH$_3$) ppm.

Anal. Calcd. for $C_{21}H_{20}O_3NSF$: C, 65.44; H, 5.23; N, 3.63. Found: C, 65.45; H, 5.23; N, 3.65.

*4.1.5. 2-((1Z)-1-(4-(Methylsulfinyl)benzylidene)-5-fluoro-2-methyl-1-*H*-inden-3-yl)-*N*-methylacetamide (**20**)*

Derivative **20** was obtained in two steps (Fischer esterification and aminolysis; see Sections 4.1.2 and 4.1.4), as yellow crystals in 50% overall yield, mp 150–152 °C.

NMR ^{1}H (200 MHz, DMSO d_6) δ: 2.20 (s, ArCH_3); 2.76 (d, J = 4.8 Hz, ArCONHCH_3); 2.80 (s, SOCH_3); 3.51 (s, ArCH_2CONHR); 5.77 (br, CON*H*); 6.58 (td, J = 8.1 Hz, 9.0 Hz and 2.1 Hz, H6); 6.84 (dd, J = 9.0 Hz and 2.1 Hz, H4); 7.16 (dd, J = 5.2 Hz and 8.1 Hz, H7); 7.65 (s, C=C*H*); 7.72 (d, J = 8.0 Hz, H2′ and H6′); 7.78 (d, J = 8.0 Hz, H3′ and H5′) ppm.

NMR ^{13}C (50 Hz, DMSO d_6) δ: 10.7 (Ar*C*H$_3$); 26.7 (CONHCH_3); 33.8 (Ar*C*H$_2$CONHCH_3); 44.0 (SOCH_3); 106.3 (C4); 111.3 (C6); 123.9 (C7); 128.8 (C=*C*H); 124.0 (C2′ and C6′); 129.7 (C2); 130.4 (C3′ and C5′); 132.8 (C1′); 139.1 (C3); 141.7 (C7a); 145.8 (C4′); 146.7 (C3a); 161.2 (C1); 166.1 (C5); 169.9 (Ar*C*ONHCH$_3$) ppm.

Anal. Calcd. for $C_{21}H_{20}O_2NSF$: C, 68.27; H, 5.46; N, 3.79. Found: C, 68.26; H, 5.47; N, 3.75.

4.2. Pharmacology

4.2.1. Antinociceptive activity

The analgesic activity was determined in vivo by the acetic acid-induced (0.6%; 0.1 mL/10 g) abdominal constriction test in mice [54]. Albino mice of both sexes (18–23 g) were used. Compounds were administered orally (300 μmol/kg) as a suspension in 5% Arabic gum in saline (vehicle). Sulindac (300 μmol/kg) was used as standard drug under the same conditions. Acetic acid solution was administered i.p. 1 h after administration of the compounds. 10 min after the i.p. acetic acid injection the number of constrictions per animal was recorded for 20 min. Control animals received an equal volume of vehicle. Antinociceptive activity was expressed as % of inhibition of constrictions when compared with the vehicle control group. Results are expressed as mean ± SEM of n animals per group. The data were statistically analyzed by the Student's t-test for a significance level of $^*p < 0.05$.

4.2.2. Anti-inflammatory activity

The anti-inflammatory activity was determined in vivo by the carrageenan-induced rat paw edema test [54]. Fasted albino rats of both sexes (150–200 g) were used. Test compounds and the anti-inflammatory standard drugs sulindac and celecoxib were administered orally at a dose of 300 μmol/kg as a suspension in 5% Arabic gum in saline (vehicle). Control animals received an equal volume of vehicle. 1 h later, the animals were then injected with either 0.1 mL of 1% carrageenan solution in saline (0.1 mg/paw) or sterile saline (NaCl 0.9%) into the subplantar surface of one of the hind paw, respectively. The paw volumes were measured using a glass plethysmograph coupled to a peristaltic pump, 3 h after the subplantar administration of carrageenan. The edema was calculated as the volume variation between the injected paw with carrageenan and the saline-treated paw. The anti-inflammatory activity was expressed as % of inhibition of the edema when compared with vehicle control group. Results are expressed as mean ± SEM of n animals per group. The data were statistically analyzed by the Student's t-test for a significance level of $^*p < 0.05$.

4.2.3. Gastric ulcerogenic potential

Ulcerogenic effects were investigated as described earlier [52] in the same animals that were submitted to the anti-inflammatory evaluation. Briefly, animals were euthanized at the end of the experiments and the stomachs excised along its greater curvature for visualization of gastric lesions with a stereomicroscope.

4.3. Molecular modeling

4.3.1. Selection of protein crystal structures

Ligand-bound crystallographic structures of COX-1 and COX-2 are available in the Protein Data Bank [63]. In this study, COX-1 crystal structures 1PXX, 3PGH, 1Q4G, 1HT8 and COX-2 crystal structures 1CX2, 4COX, 6COX were evaluated and selected for docking [44–48].

4.3.2. Preparation of the ligands

The preparation of the ligands for FLExE was performed as for FLExX [64] using Sybyl version 7.3 [65]. First, the ligand coordinates were generated using the program Sketcher, available in Sybyl version 7.3. Next, the correct atom types (including hybridization states) and correct bond types were defined, hydrogen atoms were added, charges were assigned to each atom, and finally the structures were energy-minimized. All carboxylic acid groups were modeled in their ionized forms. The energies of ligand structures were previously minimized using the semiempirical AM1 method [66] with PC Spartan v.04 software [67]. PM3 point charges were assigned to the ligands [58].

4.3.3. Preparation of the ensemble protein structures

Proteins were prepared for the docking studies using the Biopolymer module of Sybyl 7.3. Amber7 FF99 charges were

attributed to the protein atoms [68]. The first step in the generation of suitable protein structures for the ensemble superimposition is the deletion of extra chains. In this work, chains A were kept while the others were deleted. Next, Biopolymer protein analysis tool was used, in a stepwise process of analysis and correction of geometry parameters. For each structure, the description of an ensemble contains the definition of the protein atoms, the resolution of ambiguities in the PDB file, the location of hydrogen atoms at hetero atoms, and the definition of the active site atoms. The assignment of hydrogen positions has been made on the basis of default rules. The side-chains of lysine, arginine and the carboxylate groups of aspartic and glutamic acids have been modeled in their ionized states. Water molecules contained in the PDB file have been removed. Finally, the active site of the ensemble has been defined as the collection of residues within 10.0 Å of the bound inhibitor and comprised the union of all ligands of the ensemble. All atoms located less than 10.0 Å from any ligand atom were considered. 1PXX was used as a reference structure for the united protein preparation in COX-1 studies, while 1CX2 was used as a reference in COX-2 studies.

4.3.4. Lipinski's rule of five

CLOGP, the log of the octanol/water partition coefficient, was calculated with the CLOGP software [62]. PSA and molecular weight calculations have been performed with the MOLPROP facility, available in the QSAR module of Sybyl 7.3 [65].

Acknowledgements

The authors wish to thank IM-INOFAR (#420.015/2005-1, Br), PRONEX (Br), CNPq (Br), FAPERJ (Br), FUJB (Br) for financial support and fellowships (to ALPM, EJB, CAMF and NCR).

References

[1] J.R. Vane, Nature 231 (1971) 232–235.
[2] P.M. Brooks, R.O. Day, New Engl. J. Med. 324 (1991) 1716–1725.
[3] J.Y. Fu, J.L. Masferrer, K. Seibert, A. Raz, P.J. Needleman, Biol. Chem. 265 (1990) 16737–16740.
[4] W. Xie, J.G. Chipman, D.L. Robertson, R.L. Erikson, D.L. Simmons, Proc. Natl. Acad. Sci. 88 (1991) 2692–2696.
[5] J.A. Mitchell, P. Akarasereenont, G. Thiemermann, R.J. Flower, J.R. Vane, Proc. Natl. Acad. Sci. 90 (1993) 11693–11697.
[6] J.R. Vane, R.M. Botting, Inflamm. Res. 44 (1995) 1–10.
[7] D.L. Simmons, R.M. Botting, T. Hla, Pharmacol. Rev. 56 (2004) 387–437.
[8] D.E. Duggan, K.F. Hooke, E.A. Risley, T.Y. Shen, C.G. Arman, Pharmacol. Exp. Ther. 201 (1977) 8–13.
[9] W.E. Sneader, Br. Med. J. 321 (2000) 1591–1594.
[10] E.A. Meade, W.L. Smith, D.L. DeWitt, J. Biol. Chem. 268 (1993) 6610–6614.
[11] T.Y. Shen, R.L. Ellis, T.B. Windholz, A.R. Matzuk, A. Rosegay, S. Lucas, B.E. Witzel, C.H. Stammer, A.N. Wilson, F.W. Holly, J.B. Willett, L.H. Sarett, W.J. Holtz, C.A. Winter, E.A. Risley, G.W. Nuss, J. Am. Chem. Soc. 85 (1963) 488–489.
[12] A. Zarghi, P.N.P. Rao, E.E. Knaus, Bioorg. Med. Chem. 15 (2007) 1056–1061.
[13] M. Biava, G.C. Porretta, G. Poce, S. Supino, S. Forli, M. Rovini, A. Cappelli, F. Manetti, M. Botta, L. Sautebin, A. Rossi, C. Pergola, C. Ghelardini, E. Vivoli, F. Makovec, P. Anzellotti, P. Patrignani, M. Anzini, J. Med. Chem. 50 (2007) 5403–5411.
[14] W.C. Black, C. Brideau, C.-C. Chan, S. Charleson, N. Chauret, D. Claveau, D. Ethier, R. Gordon, G. Greig, J. Guay, G. Hughes, P. Jolicoeur, Y. Leblanc, D. Nicoll-Griffith, N. Ouimet, D. Riendeau, D. Visco, Z. Wang, L. Xu, P. Prasit, J. Med. Chem. 42 (1999) 1274–1281.
[15] F. Julemont, X. de Leval, C. Michaux, J.-F. Renard, J.-Y. Winum, J.-L. Montero, J. Damas, J.-M. Dogne, B. Pirotte, J. Med. Chem. 47 (2004) 6749–6759.
[16] T.D. Penning, J.J. Talley, S.R. Bertenshaw, J.S. Carter, P.W. Collins, S. Docter, M.J. Graneto, L.F. Lee, J.W. Malecha, J.M. Miyashiro, R.S. Rogers, D.J. Rogier, S.S. Yu, G.D. Anderson, E.G. Burton, J.N. Cogburn, S.A. Gregory, C.M. Koboldt, W.E. Perkins, K. Seibert, A.W. Veenhuizen, Y.Y. Zhang, P.C. Isakson, J. Med. Chem. 40 (1997) 1347–1365.
[17] X. De Leval, F. Julemont, V. Benoit, M. Frederich, B. Pirotte, J.M. Dogne, Mini Rev. Med. Chem. 4 (2004) 597–601.
[18.] J.J. Talley, D.L. Brown, J.S. Carter, M.J. Graneto, C.M. Koboldt, J.L. Masferrer, W.E. Perkins, R.S. Rogers, A.F. Shaffer, Y.Y. Zhang, B.S. Zweifel, K. Seibert, J. Med. Chem. 43 (2000) 775–777.
[19] D. Riendeau, M.D. Percival, C. Brideau, S. Charleson, D. Dubé, D. Ethier, J.P. Falgueyret, R.W. Friesen, R. Gordon, G. Greig, J. Pharmacol. Exp. Ther. 296 (2001) 558–566.
[20] J.M. Dogne, C.T. Supuran, D. Pratico, J. Med. Chem. 48 (2005) 2251–2257.
[21] D.H. Solomon, Arthritis Rheum. 52 (2005) 1968–1978.
[22] B. Arun, P. Goss, Semin. Oncol. 2 (2004) 22–29.
[23] L.R. Howe, Breast Cancer Res. 9 (2007) 210.
[24] R.E. Harris, J. Beebe-Donk, G.A. Alshafie, BMC Cancer 6 (2006) 27–31.
[25] R.E. Harris, J. Beebe-Donk, H. Doss, D. Burr Doss, Oncol. Rep. 13 (2005) 559–583.
[26] D.W. McFadden, D.R. Riggs, B.J. Jackson, C. Cunningham, Int. J. Oncol. 29 (2006) 1019–1023.
[27] M.M. Taketo, J. Natl. Cancer Inst. 90 (1998) 1529–1536.
[28] M.M. Taketo, J. Natl. Cancer Inst. 90 (1998) 1609–1620.
[29] N. Babbar, N.A. Ignatenko, R.A. Casero Jr., E.W. Gerner, J. Biol. Chem. 278 (2003) 47762–47775.
[30] G.A. Piazza, D.S. Alberts, L.J. Hixson, N.S. Paranka, H. Li, T. Finn, C. Bogert, J.M. Guillen, K. Brendel, P.H. Gross, G. Sperl, J. Ritchie, R.W. Burt, L. Ellsworth, D.J. Ahnen, R. Pamukcu, Cancer Res. 57 (1997) 2909–2915.
[31] A.S. Kalgutkar, A.B. Marnett, B.C. Crews, R.P. Remmel, L.J. Marnett, J. Med. Chem. 43 (2000) 2860–2870.
[32] A.S. Kalgutkar, B.C. Crews, S. Saleh, D. Prudhomme, L.J. Marnett, Bioorg. Med. Chem. 13 (2005) 6810–6822.
[33] S. Khanna, M. Madan, A. Vangoori, R. Banerjee, R. Thaimattam, S.K. Jafar Sadik Basha, M. Ramesh, S.R. Casturi, M. Pal, Bioorg. Med. Chem. 14 (2006) 4820–4833.
[34] A.S. Kalgutkar, B.C. Crews, S.W. Rowlinson, A.B. Marnett, K.R. Kozak, R.P. Remmel, L.J. Marnett, Proc. Natl. Acad. Sci. USA 97 (2000) 925–930.
[35] A.S. Kalgutkar, S.W. Rowlinson, B.C. Crews, L.J. Marnett, Bioorg. Med. Chem. Lett. 12 (2002) 521–524.
[36] E.J. Barreiro, M.E. Lima, Braz. J. Med. Biol. Res. 22 (1989) 1415–1419.
[37] E. Gourzoulidou, M. Carpintero, P. Baumhof, A. Giannis, H. Waldmann, ChemBioChem 6 (2005) 527–531.
[38] D.E. Duggan, K.F. Hooke, S.S. Hwang, Drug Metab. Dispos. 8 (1980) 241–246.
[39] J.T. Lim, G.A. Piazza, E.K. Han, T.M. Delohery, H. Li, T.S. Finn, R. Buttyan, H. Yamamoto, G.J. Sperl, K. Brendel, P.H. Gross, R. Pamukcu, I.B. Weinstein, Biochem. Pharmacol. 58 (1999) 1097–1107.
[40] J.B. Nixon, H. Kamitanib, S.J. Baeka, T.E. Eling, Prostaglandins Leukot. Essent. Fatty Acids 68 (2003) 323–330.
[41] Y. Niitsu, T. Takayama, K. Miyanishi, A. Nobuoka, T. Hayashi, T. Kukitsu, K. Takanashi, H. Ishiwatari, T. Abe, T. Kogawa, M. Takahashi, T. Matsunaga, J. Kato, Cancer Chemother. Pharmacol. 54 (2004) S40–S43.
[42] K. Gwyn, F.A. Sinicrope, Am. J. Gastroenterol. 97 (2002) 13–21.
[43] B. Jung, V. Barbier, H. Brickner, J. Welsh, A. Fotedar, M. McClelland, Cancer Lett. 219 (2005) 15–25.
[44] S.W. Rowlinson, J.R. Kiefer, J.J. Prusakiewicz, J.L. Pawlitz, K.R. Kozak, A.S. Kalgutkar, W.C. Stallings, R.G. Kurumbail, L.J. Marnett, J. Biol. Chem. 278 (2003) 45763–45769.
[45] R.G. Kurumbail, A.M. Stevens, J.K. Gierse, J.J. McDonald, R.A. Stegeman, J.Y. Pak, D. Gildehaus, J.M. Miyashiro, T.D. Penning, K. Seibert, P.C. Isakson, W.C. Stallings, Nature 384 (1996) 644–648.
[46] K. Gupta, B.S. Selinsky, C.J. Kaub, A.K. Katz, P.J. Loll, J. Mol. Biol. 335 (2004) 503–518.
[47] B.S. Selinsky, K. Gupta, C.T. Sharkey, P.J. Loll, Biochemistry 40 (2001) 5172–5180.
[48] P.J. Loll, D. Picot, O. Ekabo, R.M. Garavito, Biochemistry 35 (1996) 7330–7340.
[49] H. Claußen, C. Buning, M. Rarey, T. Lengauer, J. Mol. Biol. 308 (2001) 377–395.
[50] C.A. Lipinski, F. Lombardo, B.W. Dominy, P.J. Feeney, Adv. Drug Deliv. Rev. 46 (2001) 3–25.
[51] B.M. Trost, D.P. Curran, Tetrahedron Lett. 22 (1981) 1287–1290.
[52] T. Barf, J. Vallgarda, R. Emond, C. Häggström, E. Mosialou, K. Axelsson, R. Olsson, L. Engblom, N. Edling, Y. Rönquist-Nii, B. Öhman, P. Alberts, L. Abrahmsén, J. Med. Chem. 45 (2002) 3813–3815.
[53] N.D. Karis, W.A. Loughlin, I.D. Jenkins, Tetrahedron 63 (2007) 12303–12309.
[54] I.G. Ribeiro, K.C.M. Silva, S.C. Parrini, A.L.P. Miranda, C.A.M. Fraga, E.J. Barreiro, Eur. J. Med. Chem. 33 (1998) 225–235.
[55] C.C. Chan, S. Boyce, C. Brideau, A.W. Fordhutchinson, R. Gordon, D. Guay, R.G. Hill, C.S. Li, J. Mancini, M. Penneton, J. Pharmacol. Exp. Ther. 274 (1995) 1531–1537.
[56] L.M. Lima, E.J. Barreiro, Curr. Med. Chem. 12 (2005) 23–49.
[57] V. Quidville, N. Segond, S. Lausson, M. Frenkian, R. Cohen, A. Jullienne, Prostaglandins Other Lipid Mediat. 81 (2006) 14–30.
[58] J.J.P. Stewart, J. Comput. Chem. 10 (1989) 209–220.
[59] R. Pouplana, J.J. Lozano, C. Pérez, J. Ruiz, J. Comput. Aided Mol. Des. 16 (2002) 683–709.
[60] J.R. Kiefer, J.L. Pawlitz, K.T. Moreland, R.A. Stegeman, W.F. Hood, J.K. Gierse, A.M. Stevens, D.C. Goodwin, S.W. Rowlinson, L.J. Marnett, W.C. Stallings, R.G. Kurumbail, Nature 405 (2000) 97–101.
[61] D.E. Clark, S.D. Pickett, DDT 5 (2000) 49–57.
[62] J. Chow, P. Jurs, J. Chem. Inf. Comput. Sci. 19 (1979) 172–178.

[63] H.M. Berman, J. Westbrook, Z. Feng, G. Gilliland, T.N. Bhat, H. Weissig, I.N. Shindyalov, P.E. Bourne, Nucleic Acids Res. 28 (2000) 235–242.
[64] M. Rarey, B. Kramer, T. Lengauer, G.A. Klebe, J. Mol. Biol. 261 (1996) 470–489.
[65] SYBYL 7.3 ed., Tripos Inc., 1699 South Hanley Rd., St. Louis, Missouri, 63144, USA; http://www.tripos.com.
[66] M.J.S. Dewar, E.G. Zoebisch, E.F. Healy, J.J.P. Stewart, J. Am. Chem. Soc. 107 (1985) 3902–3909.
[67] (a) Spartan´04; Wavefunction Inc., 18401 Von Karman Avenue, Suite 370. Irvine, California 92612, USA.
(b) PC SPARTAN Pro User's Guide, Wavefunction Inc., California.
[68] D.A. Case, D.A. Pearlman, J.W. Caldwell, T.E. Cheatham III, J. Wang, W.S. Ross, C.L. Simmerling, T.A. Darden, K.M. Merz, R.V. Stanton, A.I. Cheung, J.J. Vincent, M. Crowley, V. Tsui, H. Gohike, R.J. Radmer, Y. Duan, J. Pitera, I. Massova, G.L. Seibel, U.C. Singh, P.K. Weiner, P.A. Kollman, Amber 7, University of California, San Francisco, 2002.